Nanoscale

Dynamic Article Links ►

Cite this: Nanoscale, 2013, 5, 3733

PAPER

Surface-modified multifunctional MIP nanoparticles

Ewa Moczko, Alessandro Poma, Antonio Guerreiro*, Isabel Perez de Vargas Sansalvador, Sarah Caygill, Francesco Canfarotta, Michael J. Whitcombe, Sergey Piletsky

DOI: 10.1039/c3nr00354j

The synthesis of core-shell molecularly imprinted polymer nanoparticles (MIP NPs) has been performed using a novel solid-phase approach on immobilised templates. The same solid phase also acts as protective functionality for high affinity binding sites during subsequent derivatisation/shell formation. This procedure allows for the rapid synthesis, controlled separation and purification of high-affinity materials, with each production cycle taking just 2 hours. The aim of this approach is to synthesise uniformly-sized imprinted materials at the nanoscale which can be readily grafted with various polymers without affecting their affinity and specificity. For demonstration purposes we grafted anti-melamine MIP NPs with coatings which introduce the following surface characteristics: high polarity (PEG methacrylate); electro-activity (vinyl ferrocene); fluorescence (eosin acrylate); thiol groups (pentaerythritol *tetrakis*(3-mercaptopropionate)). The method has broad applicability and can be used to produce multifunctional imprinted nanoparticles with potential for further application in the biosensors, diagnostics and biomedical fields and as an alternative to natural receptors.

Introduction

Molecular imprinting of polymers has attracted widespread interest as a technique for the production of robust and highly selective synthetic receptors for a variety of small molecules.[1-3] This process relies on the formation of a complex between functional monomers and template molecules through either covalent or non-covalent interactions, followed by polymerisation with suitable cross-linking monomers. The resulting polymers, or MIPs (Molecularly Imprinted Polymers), following template removal, contain template-shaped cavities with spatial distribution of functional groups complementary to the imprinted target. The presence of these cavities allows for subsequent selective recognition of the target or related structural analogues.

Over the years different approaches have been applied to the production of MIPs, mostly in the form of bulk materials. MIPs are conventionally synthesised as monoliths followed by lengthy grinding, sieving and extended washings to remove template. The final products obtained in this way are small fragments with irregular shapes and sizes. Although progress has been made in this field, no significant improvement has been reported considering their practical application and the possibility for integration of MIPs in biosensors and assays. Moreover, polymers prepared by conventional routes (monoliths) are not suitable for standard industrial manufacturing and production processes.[4, 5] In order to advance the implementation of MIPs in sensors and assays they should be synthesised in different formats, ideally as soluble or colloidal nanoparticles.

Research associated with the development of smart materials operating at the nanometer scale has increased noticeably in recent years.[6-10] Nanoparticles offer significant advantages over traditional bulk materials due to their high external surface area to volume ratio, which results in increased chemical reactivity, capacity and fast binding kinetics. Physical and chemical properties, including uniform spherical geometry, stability and ease of dispersion, make them attractive for integration with biochips and microarrays, for use in molecular diagnostic (nanoscale analysis) or point of care delivery (by injection, inhalation etc.).[11-13]

Imprinted polymer nanoparticles (MIP NPs) with high affinity and selectivity for their target analytes have attracted considerable interest as potential substitutes for typical biological recognition elements such as antibodies and enzymes.[2, 5, 14, 15] However, the simple recognition (binding) of the target molecule by the MIP NP is insufficient for the majority of practical applications which requires the particle to possess one or more additional characteristics. These could be incorporated by the inclusion of suitable specialist monomers in the original polymerisation mixture; however this is not always feasible, since they may not be compatible with the imprinting process. For this reason surface modification of NPs is extremely desirable; examples include: the attachment of fluorescent or electro-active tags to aid transduction in sensing application or in assays; surface functionalities to enable the immobilisation of particles in device manufacture; the improvement of surface characteristics (such as biocompatibility or to prevent particle aggregation) or the introduction of catalytic properties. The availability of such functionalised MIP NPs would enable the manufacture of inexpensive, stable and reliable devices based on smart nanomaterials. These can be particularly advantageous in areas such as analytical or biomedical diagnostics,[7, 16, 17] controlled

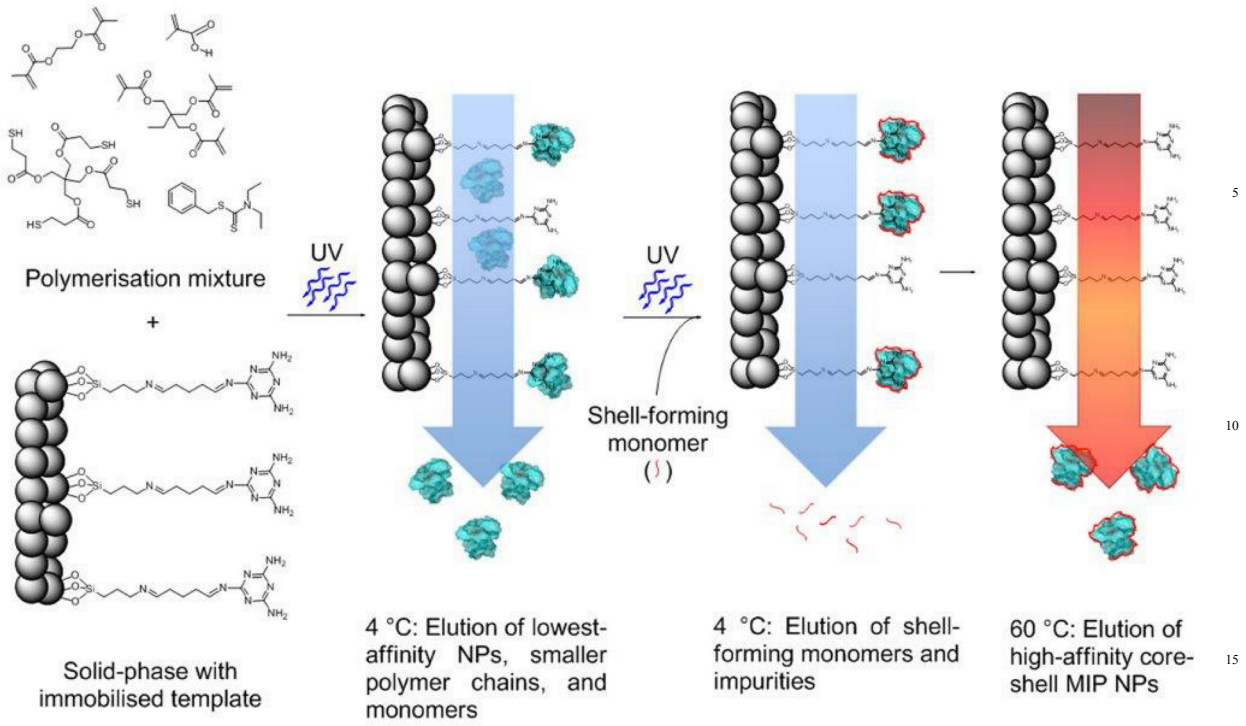

Fig. 1 Schematic representation of the solid-phase synthesis and selection of core-shell MIP NPs.

drug delivery,[18-20] biosensors,[21, 22] chromatography, solid-phase extraction (SPE) and even antidotes for toxins and viruses.[23, 24] Here we demonstrate the general concept of a new approach to the production of MIP NPs and their subsequent post-derivatisation with a thin grafted layer of polymeric material that differs from the nanoparticles core[25, 26] which can be used to modify its electronic, magnetic, mechanical or optical behaviour. The method relies on the formation of the imprinted nanoparticles in the presence of template molecules immobilised on the surface of a solid support, which after synthesis, doubles as affinity matrix for the retention of high affinity particles. These remain attached to the solid support via their interaction with the template, allowing post-derivatisation of the exposed surface of the NPs. The presence of the template within the binding site and its proximity to the surface of the solid support ensures that the binding sites are protected during the grafting process. The synthesis of core-shell MIP NPs using this method is represented schematically in Fig. 1. A polymerisation mixture comprising functional monomer, cross-linker and iniferter, dissolved in a suitable solvent are loaded onto a solid support where the template has been previously immobilised. Polymerisation is initiated using UV irradiation. After synthesis, unreacted monomers and low affinity particles are eluted from the solid-phase at low temperature whilst the high affinity particles remain bound to the template. The level of their affinity is a result of interactions with template molecules and therefore the stability of the complex formed between particles and the template. Thus, particles formed in solution (away from the template) or with improperly formed binding sites will naturally have lower affinity and be eluted in this cold wash. The high affinity particles are subsequently grafted with a suitable secondary monomer (e.g. one containing fluorescent or electro-active groups) by the introduction of a solution of this monomer to the solid phase and the application of UV light (post-irradiation). After polymerisation of the shell and subsequent washing steps, the temperature of the solvent is increased, allowing elution of the high affinity core-shell MIP NPs. Raising the temperature increases the rate of exchange of particles with the template and reduces the strength of association, allowing them to be eluted from the solid matrix.

Experimental

Materials. Melamine (MEL), desisopropyl atrazine (DA), methacrylic acid (MAA), ethylene glycol dimethacrylate (EGDMA), trimethylolpropane trimethacrylate (TRIM), vinylferrocene (VFc), phosphate buffered saline (PBS), pentaerythritol-tetrakis-(3-mercaptopropionate) (PETMP), 3-aminopropyltrimethyloxysilane (APTMS), glutaraldehyde (GA), *N,N'*-Bis(acryloyl)cystamine (BAC), acryloyl chloride, eosin Y disodium salt, *N*-methyl-2-pyrrolidone (NMP), poly(ethylene glycol) (PEG) methacrylate (Mw = 360 g mol^{-1}), 2-(trifluoromethyl) acrylic acid (TFMAA) and toluene were purchased from Sigma-Aldrich, UK. Acetonitrile (ACN), dichloromethane (DCM), sulphuric acid, hydrogen peroxide, ethanol, sodium hydroxide, sand (40-100 mesh) and silica gel for chromatography (35μm-70μm diameter) were obtained from Fisher Scientific (UK). Amine-derivatised latex beads (258 nm diameter) were purchased from Estapor, Merck International. Methanol and acetone were purchased from VWR (UK). *N,N*-diethyldithiocarbamic acid benzyl ester was bought from TCI

Europe (Belgium). Glass beads (Spheriglass® 2429, 53 μm < diameter < 106 μm) were purchased from Blagden Chemicals, UK. Deionised water obtained from a Millipore (MilliQ) purification system at resistivity 18.2 MΩ cm was used for analysis. All chemicals were analytical or HPLC grade and were used without further purification.

Preparation of melamine-derivatised glass beads as affinity media. Glass beads (300 mL) were first shaken with ceramic beads on 45 μm sieves for 5 h using a Vibratory Sieve Shaker AS 200 basic (Retsch, UK) in order to abrade the surface coating and expose a fresh surface. After recovery from the sieve, the surface of the beads was activated by boiling with 4 M NaOH for 10 min, rinsing with deionised water and acetone, and drying at 80 °C. The dry beads were incubated overnight in 2 % v/v APTMS/toluene solution to introduce surface amino groups. After incubation, beads were rinsed with acetone and then incubated for another 2 h in 5 % v/v GA/ PBS solution at pH 7.4 and followed by washing with deionised water. The surface immobilisation of the template was performed overnight at 4 °C by incubating the beads with a solution of melamine (5 mg mL^{-1}) in PBS (pH 7.4) containing 10 % v/v of NMP, this procedure was reported to yield 2.55×10^{13} templates per cm^{-2} (Sheng and Ye, 2009).[27] Finally, the glass beads were rinsed with deionised water, dried *in vacuo* and stored at 4 °C.

Preparation of melamine-derivatised latex beads. Amine-derivatised latex beads were modified with melamine following the same protocol as above, but starting from the step of the reaction with glutaraldehyde. Purification of the modified latex beads was achieved by dialysis against water over 5 days in order to remove free melamine.

Synthesis of melamine-MIP NPs. The composition of the polymerisation mixture for the synthesis of the core MIP NPs for melamine detection was adapted from (Guerreiro et al., 2009).[1] It was prepared by mixing MAA (2.88 g) as functional monomer, EGDMA (3.24 g) and TRIM (3.24 g) as cross-linkers, *N,N*-diethyldithiocarbamic acid benzyl ester (0.753 g) as iniferter and of pentaerythritol-tetrakis-(3-mercaptopropionate) (PETMP) (0.18 g) as chain transfer agent. All compounds were dissolved in ACN (10.52 g). The mixture was placed in a glass vial and purged with N_2 for 20 min. Melamine-derivatised glass beads (30 g) were placed in a 200 mL flat-bottomed glass beaker and degassed *in vacuo* for 20 min. The polymerisation mixture was poured onto the glass beads and the vessel was placed between two UV light sources (both Philips model HB/171/A, each fitted with 4×15 W lamps) for 2 min 30 s under a continuous stream of nitrogen. After polymerisation, the contents of the beaker was transferred into an SPE cartridge fitted with a polyethylene frit (20 μm porosity) in order to perform the temperature-based affinity separation of MIP NPs. The SPE cartridge was first placed in an ice bath (0 °C) for 7 min and the supernatant was drained using a syringe piston. Washing steps were carried out at low temperature by washing with 12 bed volumes of ACN at 0 °C. Low temperature washing was performed in order to remove unpolymerized monomers and low affinity MIP NPs. The efficiency of the elution/washing process was assessed by UV spectrophotometric analysis of the column eluate. After washing at low temperature, the temperature of the SPE cartridge and of the ACN eluent was increased to 60 °C. This allowed the elution of high affinity MIP NPs from the solid-phase. This was achieved by pouring ACN into the cartridge followed by incubation at 60 °C for 4 min before collection of the eluate. This procedure was performed 6 times. The total volume of high affinity MIP NPs in ACN collected was about 150 mL.

Post-derivatisation of melamine-MIP NPs. Post-derivatisation was performed on the solid-phase (glass beads) containing the high-affinity MIP NPs attached (i.e. on material prepared as described in the preceding section after washing at low temperature but before the high temperature elution phase). For this either poly(ethylene glycol) methacrylate (150 mg), vinylferrocene (90 mg), eosin acrylate (45 mg) or PETMP (0.06 g) was dissolved in ACN (15 mL) added to a 200 mL capacity sealed glass vessel along with the glass beads with attached MIP NPs recovered from the SPE cartridge. The mixture was bubbled with N_2 for 5 min and irradiated with UV for 2 min 30 s using the same arrangement of lamps as described above. Following irradiation, the contents of the vessel were transferred into a new SPE cartridge and washing performed 12 times following the same protocol as described in the preceding section. The washing process was monitored by UV spectroscopy, in order to ensure complete removal of all unreacted monomers from the glass beads. After the washing, the hot elution step was also carried out as described in the preceding section.

Dynamic Light Scattering (DLS). Particles sizes were measured with a Zetasizer Nano (Nano-S) particle-size analyser from Malvern Instruments Ltd (UK). An aliquot of the dispersion of NPs in ACN (1 mL) was sonicated for 10 min and concentrated down to 500 μl by evaporation of the solvent under a stream of nitrogen, then diluted in 1 mL of deionised water. The dispersion was filtered through a 1.2 μm glass fibre syringe filter and analysed by DLS at 25 °C in a 3 cm^3 disposable polystyrene cuvette. The values are reported as an average of at least 3 measurements.

Transmission Electron Microscopy (TEM) analysis. TEM images were obtained on a Philips CM20 Transmission Electron Microscope. Prior to TEM analysis, samples were sonicated for 5 min before placing a drop of the sample on a carbon coated copper grid and drying in air.

Fluorescence measurements. Measurements of fluorescence intensity were performed using a Cary Eclipse spectrofluorometer (Varian Australia Pty Ltd) at 25 °C. The excitation and emission slit widths were 5 and 10 nm respectively. The fluorescence measurements were performed using 1 mL quartz cuvettes of 10 nm path length.

Cyclic voltammetry. Staircase cyclic voltammetry experiments were performed using a μAutolab Type II potentiostat (Ecochemie, Netherlands) at a scan rate of 10 mV s^{-1} between 0.0 V and +0.6 V. A standard three-electrode configuration was used at room temperature. A platinum gauze was used as counter electrode and a silver/silver chloride (Ag/AgCl) wire acted as the reference electrode. All potentials are stated with respect to the Ag/AgCl couple. A glass slide was coated with chromium then sputter-coated with gold and used as the working electrode. The NP solutions, in ACN, were interrogated electrochemically in the presence of a supporting electrolyte, (PBS pH 7.4), mixed with

the sample in the ration 1:1, v/v. The vinylferrocene monomer solution was prepared in ACN and diluted to 0.1 mM with an equal volume of PBS, pH 7.4.

Surface Plasmon Resonance (SPR). SPR experiments were carried out using a Biacore 3000 SPR system (GE Healthcare, UK). Au-coated chips (SIA Kit Au, Biacore), purchased from GE Healthcare (UK), were cleaned by immersion in Piranha solution (H_2SO_4/H_2O_2, 3:1 v/v) for 5 min, thoroughly rinsed with deionised water and left in ethanol overnight. The immobilization of the templates was performed by incubating the chips in a solution of cysteamine (0.2 mg mL^{-1} in ethanol) at 4 °C for 24 h, after which they were washed with ethanol and incubated in a 7 % v/v solution of GA in PBS pH 7.4 for 1 h. After this step, the chips were washed with PBS and immersed in a solution of MEL or DA (1.2 mg mL^{-1}) in PBS pH 7.4 containing 20 % v/v of methanol as co-solvent for 24 h at 4 °C. Afterwards chips were washed with methanol and dried in air. Once the immobilization was completed, the chips were assembled on their holders and stored under Ar at 4 °C until used. A volume of nanoparticle solution in ACN (10 mL) was first diluted with water then concentrated down to 2 mL using centrifugation cartridges (Amicon ultracentrifugal polypropylene, Ultracel membrane, 30 kDa MWCO, 15 mL, Millipore) purchased from Fisher Scientific (UK). The filtration was carried out according to the manufacturer's specification on a Sigma 3-16P bench-top centrifuge fitted with a swing-bucket rotor, using first deionised water and then PBS pH 7.4. For immobilization if PETMP-shell NP on Biacore chips (Fig. 6a) a solution of 0.5 mg mL^{-1} NP was injected sequentially onto a bare gold chip. Injection of melamine derivatised latex beads was then performed on the chip surface with PETMP NP coating (Fig. 6b), concentration of latex beads used was 1 μg mL^{-1}. For measurements on the Biacore, each solution was sonicated for 20 min, adjusted to a concentration of 0.5 mg mL^{-1}. Three consecutive injections of 100 μL were made and the sensor response was followed for 2 min after each injection. All experiments were performed using a flow rate of 35 μL min^{-1} at a temperature of 25 °C. Data were processed using BIAEvaluation Software v4.1.

Results

All core MIP NPs were prepared against melamine using the same procedure and monomer composition. The size and shape of the core particles were assessed using DLS and TEM analysis (see Fig. 2 for a representative TEM image). The diameters of the synthesised MIP NPs dispersed in MilliQ water were measured with DLS. The instrument allows an estimate of the size to be made based on fluctuations in the intensity of scattered light resulting from the motion of the particles. Calculations were performed using correlation analysis of the distribution of diffusion coefficients and the Stokes-Einstein equation.[28] This technique enables rapid characterization of nanoparticle dispersity using a simple measurement. Table 1 summarizes the particle sizes (DLS) obtained for the core and subsequently grafted particles. The DLS results are correlated with the hydrodynamic diameter of nanoparticles which may differ from that obtained from dry particles in the TEM due to swelling and solvation effects which only apply to the former measurement. The yield of core NPs was 16 mg, when 30 g of melamine-modified solid-phase was used, as described in the Experimental Section.

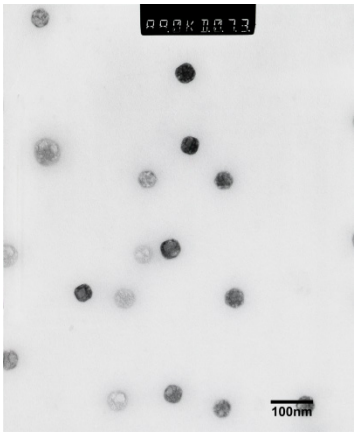

Fig. 2 TEM image of unmodified dry MIP NPs.

Table 1. Results of particle size analysis obtained by DLS for various nanoparticles preparations. (D; average hydrodynamic diameter; RSD: relative standard deviation; PDI: polydispersity index

Type of MIP NPs	D [nm]	RSD [%]	PDI
Core MIP NPs	128	1.5	0.17
postIRR-MIP NPs	116	10	0.32
PEG-MIP NPs	137	2.9	0.29
Eosin-MIP NPs	115	2.6	0.22
VFc-MIP NPs	198	1.5	0.39
PETMP-MIP NPs	212	5.2	0.38

Grafting with PEG. MIP NP cores were post-derivatised with poly(ethylene glycol) (PEG) methacrylate in ACN at 4 °C whilst still bound to the solid phase. The presence of a PEG layer in the MIP NPs was confirmed by NMR analysis. By comparing the ^{1}H-NMR spectrum obtained for MIP NPs with that of the PEGylated particles, the presence of the grafted polymer chains could be observed by the appearance of a peak in the range 3.35-3.55 ppm (data presented in Supporting Information, Figure S4).

Grafting with a fluorescent label. The modification of MIP NPs was performed through the post-irradiation of core MIP NPs with a solution of eosin *O*-acrylate in ACN. The absence of free unpolymerised eosin monomer in the high affinity fraction was confirmed by GPC analysis with fluorescence detection. The excitation and emission spectra of fluorescent MIP NPs were similar to the spectra of eosin *O*-acrylate monomer, confirming the efficiency of the grafting procedure.

Grafting of an electrochemical label. As an example, MIP NPs with an incorporated electro-active shell, poly(vinylferrocene) (pVFc) were synthesised. The core melamine MIP NPs were modified with VFc as described in the Experimental Section. The purified MIP NPs were interrogated using cyclic voltammetry. The voltammetric response of a PBS/ACN solution containing

the MIP NPs post-derivatised with pVFc displayed peaks attributed to the oxidation (E_{pa} = 0.27 V *vs* Ag/AgCl) and reduction (E_{pc} = 0.20 V *vs* Ag/AgCl) of the ferrocenyl group (Fig. 5). Peaks were observed to have shifted to a higher potential as compared to VFc, where the oxidation and reduction potentials were 0.18 V and 0.11 V *vs* Ag/AgCl, respectively.

Grafting of thiol groups. Pentaerythritol *tetrakis*(3-mercaptopropionate) (PETMP) was grafted to the surface of MIP NPs to enable them to be immobilised onto gold surfaces.[29, 30] PETMP was grafted *via* thiol-ene chemistry under UV irradiation. The efficiency of thiol grafting for immobilisation purposes was confirmed by Surface Plasmon Resonance (SPR). The binding of the thiol-modified MIP NPs to the gold surface of an SPR chip was substantially increased with respect to the un-modified core particles.

Discussion

The synthesis of MIP NPs was performed using a monomer/initiator mixture adapted from Guerreiro et al., 2009.[1] Nanoparticles were imprinted with melamine (MEL) as the template molecule which can form strong electrostatic bonds with the functional monomer methacrylic acid.[1, 31] In contrast to previous imprinting approaches, template molecules were immobilised on a solid support (Fig. 1). The synthesis was performed in the presence of a living initiator, known as an iniferter (*ini*tiator, trans*fer* agent, *ter*minator), *N,N*-diethyldithiocarbamic acid benzyl ester. This compound enables polymer chains to grow at a constant rate and prevents side reactions, such as termination of chain growth and is not subject to exothermic auto-acceleration, normally seen with non-living radical synthesis.[32] Additionally, the short irradiation times used do not result in a significant increase in the temperature of polymerisation. This helps to maintain the interactions between monomer and template during polymerisation, resulting in the formation of small homogenous nanoparticles with better-shaped imprinted cavities with higher affinity for the template.[1, 33-36] Another advantage of this approach is the ability to subsequently reinitiate polymerisation by UV irradiation, after the introduction of a secondary monomer, using macroiniferter moieties present on the surface of the nanoparticles.[32, 37] If this subsequent grafting polymerisation is carried out when the high affinity particles are still bound to the template phase, the particle surfaces can be post-functionalised whilst the binding sites are protected from modification. The average hydrodynamic diameter of the core MIP NPs was approximately 130 nm, while the same nanoparticles that had been post-irradiated in the absence of monomers for 2 min 30 s were slightly smaller, about 115 nm (see Table 1). This might be due to a higher density of cross-linking being produced during the longer subsequent irradiation time period. Post-irradiation in the presence of eosin *O*-acrylate or vinylferrocene resulted in particles with a slightly increased diameter due to the small quantity of grafted material involved in the process (see Table 1). Judging from the size we can conclude that the amount of grafted material equates to a thickness of several monomers. DLS measurements on all nanoparticles gave small standard deviations (SD) and low polydispersity index (PDI) values, which indicated a narrow size distribution in each case. The morphology of nanoparticles was evaluated using TEM analysis which confirmed that they were spherical in shape. A typical TEM image of bare MIP NPs is shown in Fig. 2. From this image particles with an average diameter of less than 100 nm could be seen. That this size differs from the results of DLS measurement (Table 1) can be explained by the fact that TEM analysis is carried out on dry particles whereas DLS measurements were made in solution where the particles may be subject to solvation effects, such as swelling.

Grafting with PEG. Initially the MIP nanoparticles produced were functionalised by grafting with PEG methacrylate. High surface energies due to the large surface area to volume ratios of nanoparticles results in enhanced chemical reactivity but can also contribute to a propensity for their aggregation. This decreases the stability in suspension and reduces the shelf-life of products containing the particles, which can interfere with their expected mode of action and present a barrier to practical applications. Coating nanoparticles with a hydrophilic polymer shell such as PEG has previously been suggested as one way to stabilize them against aggregation and render them more suitable for drug delivery and other applications *in vivo*.[7, 25, 38, 39] The stability of nanoparticles modified by grafting with PEG methacrylate in comparison to bare MIP NPs was analysed over time in aqueous suspensions using dynamic light scattering (DLS). Measurements were carried out in MilliQ water and the apparent particle size was measured on a daily basis (Fig. 3).

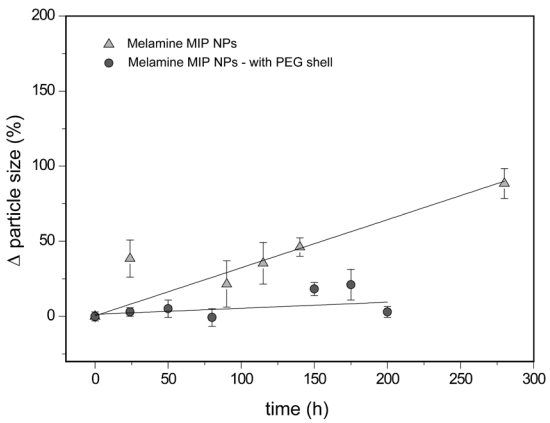

Fig. 3 Results obtained to determine the rate of aggregation of bare MIP NPs and MIP core/PEG shell NPs. Points marked as triangles (Δ) and circles (○) indicate the mean values of particle size obtained by DLS measurement as a function of time. Experiments were performed in Milli-Q water. Solid lines (—) indicate linear fits to the data points. Error bars indicate ± 1 standard deviation, n≥3.

Data points on the graph indicate how the average hydrodynamic diameter changed over time. The graph clearly shows an increase in the apparent size of core (unmodified) MIP NPs over the course of the experiment (triangles) indicative of the aggregation process. This trend is absent for particles modified by the presence of a hydrophilic shell of PEG grafted to their surface, which significantly reduces the rate of aggregation and therefore would suggest an improvement in stability when dispersed in water (circles).

Grafting of a fluorescent label. The incorporation of fluorescent compounds into MIP NPs is potentially useful for applications requiring highly sensitive detection, quantitative analysis or imaging or for chemical sensing based on changes in the fluorescence intensity of nanoparticles in response to target

binding.[2, 40, 41] One of the key challenges is the development of a suitable process for the incorporation of dyes into NPs, which would retain the intrinsic properties of the dyes, such as suitable excitation and emission wavelengths, without detrimentally influencing the specific properties of the nanoparticles.[17] We present here a procedure for the preparation of fluorescent MIP NPs coated with eosin *O*-acrylate. A schematic illustration of the synthesis of the eosin-based fluorescent monomer, a detailed description of the synthetic procedure and absorbance/emission spectra of the monomer and fluorescently-modified NPs are presented in the Supporting Information. The minor spectral shift (emission wavelength maximum shifting from 549 to 554 nm, Fig. 4) observed after grafting the fluorescent dye to the NPs was expected, demonstrating the proximity of fluorophores in the grafted layer.[42]

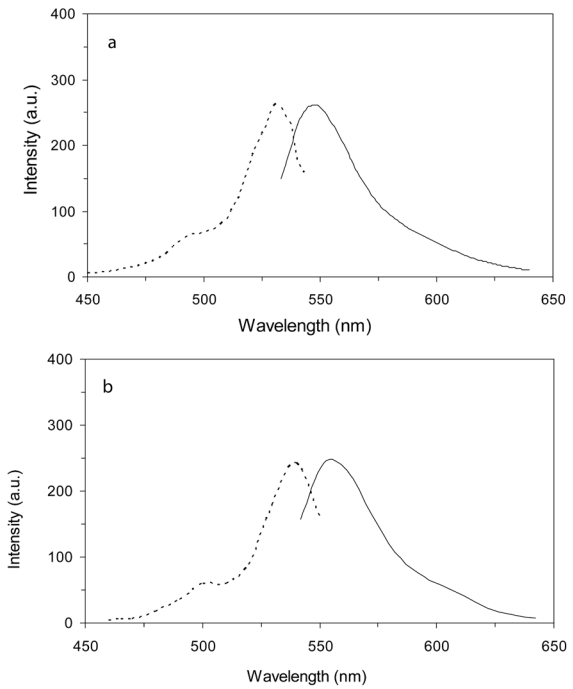

Fig. 4. Dashed line (---) indicate excitation and solid line (—) emission spectrum of (a) eosin-acrylate monomer and (b) eosin-MIP NPs at a concentration of 0.1 mg ml^{-1}.

Grafting of an electrochemical label. A number of articles have described the preparation of electrochemical (in particular amperometric) sensors and assays which employ MIP materials.[43, 44] The integration of an electro-active compound into the structure of nanoparticles represents a simple labelling technique and may provide a novel platform for the electrochemical detection of binding events. To this end MIP NPs were modified with an electro-active label by polymerisation of a vinylferrocene (VFc) shell. A comparison of the cyclic voltammogram of VFc with VFc-grafted nanoparticles is shown in Fig. 5. A shift in the oxidation/reduction couple to higher potential was observed for the nanoparticles with respect to the monomers.

The use of vinylferrocene as an electro-active polymer coating on an electrode surface also showed a shift in peak potential which is reported to be caused by several factors including the proximity of the fixed electroactive sites within the polymer shell, the presence of polymeric counter ions or the increased resistance of the electrode surface due to increased polymer deposition.[45, 46] It is likely in our case that the incorporation of vinylferrocene as a polymer shell around nanoparticles may also hinder the electrochemically-initiated redox reactions, resulting in the peak shift observed.

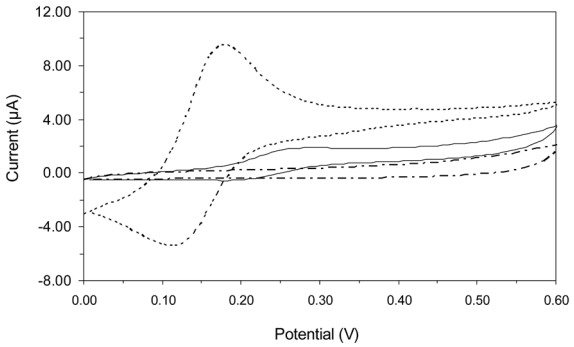

Fig. 5 Cyclic voltammograms of a 0.1 mM vinylferrocene solution (dotted line), core MIP NPs solution (dashed line) and a pVFc shell MIP NPs solution (solid line). All interrogations were performed in PBS/ACN in a 1:1 ratio. All potentials are stated with reference to the Ag/AgCl electrode.

Grafting of additional thiol groups. Whilst MIP NPs can be shown to demonstrate high affinity, selectivity and stability at low cost and with relative ease of preparation[47] they do, however, lack a simple and inexpensive means of their integration with sensor devices.[47, 48] A major challenge facing researchers developing the future practical applications of MIP materials within sensors and assays will, therefore, be related to identifying techniques for their immobilisation on the surface of transducers.[3, 49] Post-modification of nanoparticles through the grafting of suitable chemical functionalities on their surfaces may offer a promising solution to these issues of immobilisation. Thiol coupling is commonly employed for attachment of NPs to gold surfaces in sensing platforms such as SPR, QCM and in electrochemical sensors. In the case of MIP NPs, surface modification was achieved by thiol-ene chemistry with a polyfunctional mercaptan (PETMP), resulting in an increase in the number of thiol groups on the NP surface.

In order to demonstrate that the thiol-coated MIP NPs retain their affinity for melamine whilst having an increased affinity for gold surfaces, both treated and untreated nanoparticles were allowed to self-assemble on a bare gold Biacore chip. Efficient immobilisation was only observed in the case of the treated nanoparticles (Fig. 6a). This nanoparticle assembly was then challenged with latex particles coated with melamine and its response compared to the interaction of the melamine latex particles with a bare gold chip (Fig. 6b). Binding was significantly stronger to the surface coated with MIP nanoparticles compared with to the bare gold chip. This demonstrates the feasibility of using MIP NPs in biosensor applications in the same manner as antibodies are currently used.

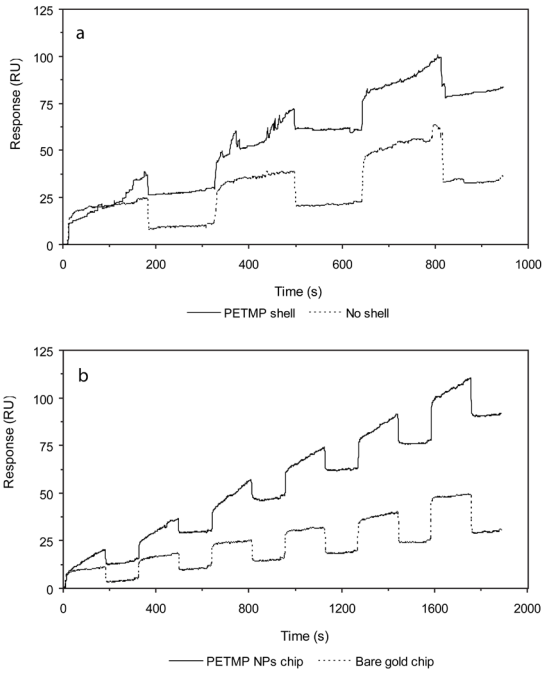

Fig. 6 SPR sensorgrams of MEL MIP NPs with PETMP shell: (a) immobilisation of bare MEL MIP NPs (dashed line) and MEL MIP NPs modified with PETMP (solid line) on gold BIAcore chip and (b) SPR sensorgrams of latex beads derivatised with melamine injected on PETMP-shell MIP NPs immobilised on a gold BIAcore chip (solid line, specific interaction) and gold chip (dashed line, non-specific interaction). The analysis was performed using PBS pH 7.4 as running buffer (flow rate: 35 µL min^{-1}) at 25 °C, injecting 100 µL sample (concentration of MIP NP was 0.5 mg mL^{-1}, concentration of melamine derivatised latex beads 1 µg mL^{-1}) and following the response for 2 min.

Effect of derivatisation on the affinity and specificity of MIP nanoparticles. It is necessary to show that the affinity and specificity of MIP NPs is not affected by the various derivatisation processes to demonstrate their suitability for a number of practical applications. The analyses were performed by SPR using the Biacore instrument. This method is ideally suited to investigate the interaction of particles with immobilised target analytes.[50] The template used in MIP synthesis, melamine, and its structural-analogue desisopropyl atrazine, were each immobilised onto the surfaces of gold chips, as described in the Experimental section.

The SPR responses due to binding of the underivatised and variously derivatised particles to immobilised melamine (target) and desisopropyl atrazine (control) chips are presented in Fig 5. Since it is possible that the functional coatings grafted to the surface of NPs could contribute to non-specific binding, it is essential to compare the interaction of NPs to both the template and its analogue. As can be seen from Fig. 7 all derivatised particles, with the exception of those grafted with PEG, show preferential binding to melamine over its analogue. The magnitude of the sensor response varied in each case, but it is possible to conclude that the derivatisation process did not adversely affect the fidelity of specific binding sites on account of the template performing the role of a "protecting group" during the derivatisation process.

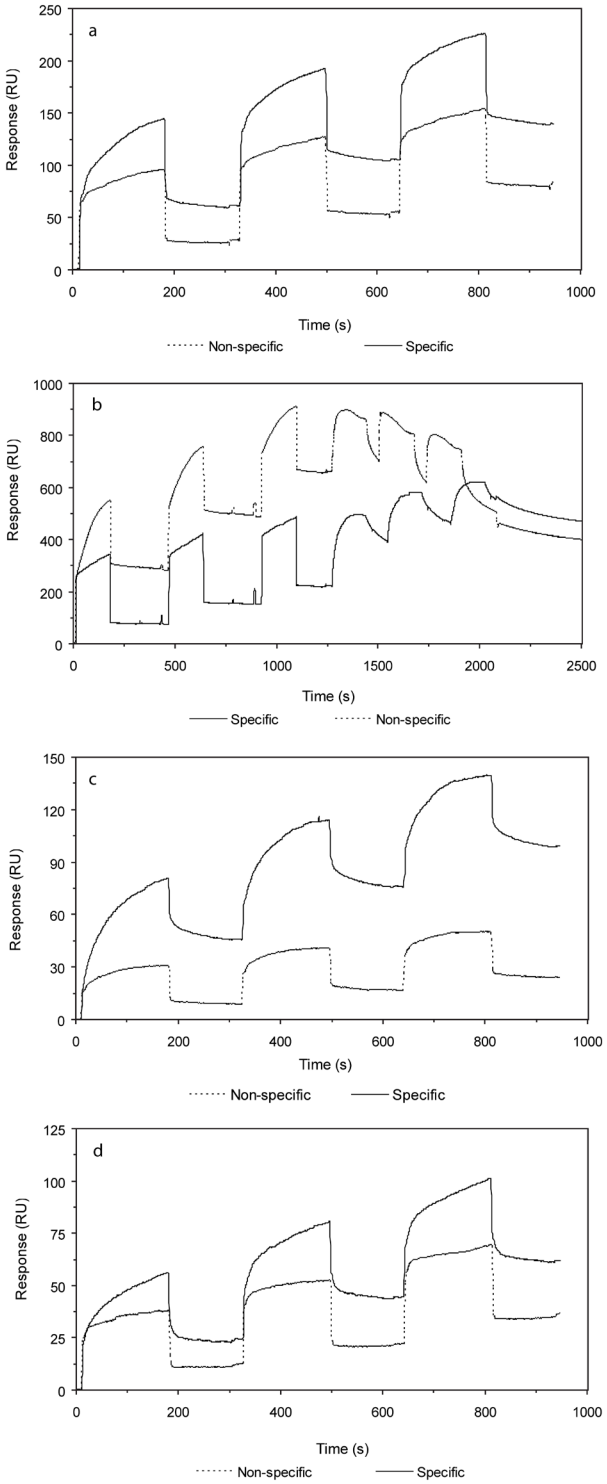

Fig. 7 SPR sensorgrams of MEL MIP NPs: (a) core MIP NPs, (b) MIP NPs with PEG shell, (c) MIP NPs with eosin shell and (d) MIP NPs with pVFc shell. Analysis was performed using Biacore with immobilised melamine (specific, solid lines) and desisopropyl atrazine (non-specific, dashed line) on gold chips. Measurements were carried out in PBS pH 7.4 as running buffer (flow rate: 35 µL min^{-1}) at 25 °C, each injection comprising 100 µL of 0.5 mg mL^{-1} solution of MIP NPs, following the response for 2 min. In the case of PEG, the first three injections are of a solution of the MIP NPs and the following three injections are of a solution of Tween 20, 0.005 % v/v.

Grafting with PEG methacrylate increased binding to both the specific and non-specific surfaces. It is difficult to provide an explanation for this phenomenon, but we can speculate that this may be an effect of increased hydrophobic binding, possibly from the apolar carbon-carbon backbone produced during formation of *poly*-PEG shell. Evidence for this is provided by the significant drop in the binding of the particles modified with PEG to desisopropyl atrazine when Tween 20 was introduced into the system (Fig. 7b).This is a well-known method of reducing the strength of hydrophobic interaction between ligands and surfaces. Interestingly, the addition of Tween did not affect the specific binding of MIP NPs to melamine, proving that specific interactions between NP and its target molecule still take place.

Conclusions

This article describes a novel method for the preparation of surface-modified imprinted nanoparticles. The protocol is based on solid-phase synthesis and subsequent derivatisation of MIP nanoparticles; it offers significant advantages for the production of multifunctional affinity materials with integrated reporter, stabiliser or biocompatible coatings. Obvious advantages include: the ease of surface modification and functionalisation; the product is obtained in pure form; low cost and high speed of manufacture, as well as protection of the specific binding sites during derivatisation. The protocol, which allows for adjustment of the monomer composition and type of grafted functionalities, can be used to address the requirements of a whole range of practical applications, such as biosensor fabrication, stability in solution/storage or even prospective *in vivo* use.

Acknowledgements

This work was supported by the Wellcome Trust with a Translation Award and by the Research Executive Agency (REA) of the European Union under Grant Agreement number PITN-GA-2010-264772 (ITN CHEBANA)

Notes and references

Cranfield Health, Cranfield University, Cranfield, Bedfordshire MK43 0AL, UK. Address correspondence to a.guerreiro@cranfield.ac.uk

† Electronic Supplementary Information (ESI) available: [details of the synthesis of eosin O-acrylate monomer and ^{1}H-NMR spectrum of MIP NPs post-derivatised with PEG shell]. See DOI: 10.1039/b000000x/

1 A. R. Guerreiro, I. Chianella, E. Piletska, M. J. Whitcombe and S. A. Piletsky, *Biosens. Bioelectron.*, 2009, **24**, 2740–2743.
2 K. Haupt, *Nat. Mater.*, 2010, **9**, 612–614.
3 G. Vasapollo, R. Del Sole, L. Mergola, M. R. Lazzoi, A. Scardino, S. Scorrano and G. Mele, *Int. J. Mol. Sci.*, 2011, **12**, 5908–5945.
4 Y. Fuchs, O. Soppera and K. Haupt, *Anal. Chim. Acta*, 2012, **717**, 7–20.
5 B. T. S. Bui and K. Haupt, *Anal. Bioanal. Chem.*, 2010, **398**, 2481–2492.
6 A. Poma, A. P. F. Turner and S. A. Piletsky, *Trends Biotechnol.*, 2010, **28**, 629–637.
7 N. Doshi and S. Mitragotri, *Adv. Funct. Mater.*, 2009, **19**, 3843–3854.
8 L. Ye and K. Mosbach, *Chem. Mat.*, 2008, **20**, 859–868.
9 S. Y. Wei, Q. Wang, J. H. Zhu, L. Y. Sun, H. F. Lin and Z. H. Guo, *Nanoscale*, 2011, **3**, 4474-4502.
10 W. Schartl, *Nanoscale*, 2010, **2**, 829–843.
11 K. K. Jain, *Clin. Chem.*, 2007, **53**, 2002–2009.
12 S. Parveen, R. Misra and S. K. Sahoo, *Nanomed.-Nanotechnol. Biol. Med.*, 2012, **8**, 147–166.
13 Y. Diebold and M. Calonge, *Prog. Retin. Eye Res.*, 2010, **29**, 596–609.
14 O. Hayden, P. A. Lieberzeit, D. Blaas and F. L. Dickert, *Adv. Funct. Mater.*, 2006, **16**, 1269–1278.
15 Z. W. Mao, H. L. Xu and D. Y. Wang, *Adv. Funct. Mater.*, 2010, **20**, 1053–1074.
16 T. Doussineau, M. Smaihi and G. J. Mohr, *Adv. Funct. Mater.*, 2009, **19**, 117–122.
17 D. L. Shi, *Adv. Funct. Mater.*, 2009, **19**, 3356–3373.
18 C. F. Nostrum, *Drug Discov Today Tech*, 2005, **2**, 119–124.
19 N. X. Wang and H. A. von Recum, *Macromol. Biosci.*, 2011, **11**, 321–332.
20 S. Grund, M. Bauer and D. Fischer, *Adv. Eng. Mater.*, 2011, **13**, B61–B87.
21 B. Pérez-López and A. Merkoçi, *Adv. Fun. Mat.*, 2011, **21**, 255–260.
22 J. L. Yan, M. C. Estevez, J. E. Smith, K. M. Wang, X. X. He, L. Wang and W. H. Tan, *Nano Today*, 2007, **2**, 44–50.
23 Y. Hoshino, H. Koide, T. Urakami, H. Kanazawa, T. Kodama, N. Oku and K. J. Shea, *J. Am. Chem. Soc.*, 2010, **132**, 6644.
24 Z. Y. Zeng, Y. Hoshino, A. Rodriguez, H. S. Yoo and K. J. Shea, *ACS Nano*, 2010, **4**, 199–204.
25 S. R. Carter and S. Rimmer, *Adv. Funct. Mater.*, 2004, **14**, 553–561.
26 N. Pérez-Moral and A. G. Mayes, *Macro. Rap. Commun.*, 2007, **28**, 2170–2175.
27 H. Sheng and B. C. Ye, *Appl. Biochem. Biotechnol.*, 2009, **152**, 54–65.
28 W. Tscharnuter, in *Encyclopedia of Analytical Chemistry*, ed. R. A. Meyers, John Wiley & Sons Ltd, Chichester, 2006, pp. 5469–5485.
29 J. C. Love, L. A. Estroff, J. K. Kriebel, R. G. Nuzzo and G. M. Whitesides, *Chem. Rev.*, 2005, **105**, 1103–1169.
30 S. Shahrokhian, A. Mahdavi-Shakib, M. Ghalkhani and R. S. Saberi, *Electroanalysis*, 2012, **24**, 425–432.
31 M. Li, L. Y. Zhang, Z. H. Meng, Z. Y. Wang and H. Wu, *J. Chromatogr. B*, 2010, **878**, 2333–2338.
32 A. R. Kannurpatti, S. X. Lu, G. M. Bunker and C. N. Bowman, *Macromolecules*, 1996, **29**, 7310–7315.
33 K. Haupt, *Anal. Chem.*, 2003, **75**, 376A–383A.
34 S. A. Piletsky, E. V. Piletska, K. Karim, K. W. Freebairn, C. H. Legge and A. P. F. Turner, *Macromolecules*, 2002, **35**, 7499–7504.
35 I. Mijangos, F. Navarro-Villoslada, A. Guerreiro, E. Piletska, I. Chianella, K. Karim, A. Turner and S. Piletsky, *Biosens. Bioelectron.*, 2006, **22**, 381–387.
36 S. A. Piletsky, A. Guerreiro, E. V. Piletska, I. Chianella, K. Karim and A. P. F. Turner, *Macromolecules*, 2004, **37**, 5018–5022.
37 T. Otsu, *J. Polym. Sci. Pol. Chem.*, 2000, **38**, 2121–2136.
38 B. A. Rozenberg and R. Tenne, *Prog. Polym. Sci.*, 2008, **33**, 40–112.
39 H. Otsuka, Y. Nagasaki and K. Kataoka, *Adv. Drug Deliv. Rev.*, 2003, **55**, 403–419.
40 M. H. Lee, Y. C. Chen, M. H. Ho and H. Y. Lin, *Anal. Bioanal. Chem.*, 2010, **397**, 1457–1466.
41 R. Y. Liu, G. J. Guan, S. H. Wang and Z. P. Zhang, *Analyst*, 2011, **136**, 184–190.
42 A. P. Demchenko, ed., *Molecular Constructions, Polymers and Nanoparticles*, Springer, Berlin, 2010.
43 T. Y. Wang and C. Shannon, *Anal. Chim. Acta*, 2011, **708**, 37–43.
44 G. J. Guan, B. H. Liu, Z. Y. Wang and Z. P. Zhang, *Sensors*, 2008, **8**, 8291–8320.
45 W. S. Schlindwein, A. Kavvada, R. J. Latham and R. G. Linford, *Polym. Int.*, 2000, **49**, 953–959.
46 G. Inzelt and L. Szabo, *Electrochim. Acta*, 1986, **31**, 1381–1387.
47 M. J. Whitcombe, I. Chianella, L. Larcombe, S. A. Piletsky, J. Noble, R. Porter and A. Horgan, *Chem. Soc. Rev.*, 2011, **40**, 1547–1571.
48 C. Malitesta, E. Mazzotta, R. A. Picca, A. Poma, I. Chianella and S. A. Piletsky, *Anal. Bioanal. Chem.*, 2012, **402**, 1827–1846.
49 Y. Ge and A. P. F. Turner, *Chem.-Eur. J.*, 2009, **15**, 8100–8107.
50 E. V. Piletska and S. A. Piletsky, *Langmuir*, 2010, **26**, 3783–3785.

